



# Cardiac troponin T and autoimmunity in skeletal muscle aging

Tan Zhang · Xin Feng · Juan Dong · Zherong Xu · Bo Feng · Karen M. Haas · Peggy M. Cawthon · Kristen M. Beavers · Barbara Nicklas · Stephen Kritchevsky

Received: 2 September 2021 / Accepted: 5 January 2022 / Published online: 15 January 2022  
© The Author(s), under exclusive licence to American Aging Association 2022

**Abstract** Age-related muscle mass and strength decline (sarcopenia) impairs the performance of daily living activities and can lead to mobility disability/limitation in older adults. Biological pathways in muscle that lead to mobility problems have not been fully elucidated. Immunoglobulin G (IgG) infiltration in muscle is a known marker of increased fiber membrane permeability and damage vulnerability, but whether this translates to impaired function is unknown. Here, we report that IgG1 and

IgG4 are abundantly present in the skeletal muscle (vastus lateralis) of ~50% (11 out of 23) of older adults (> 65 years) examined. Skeletal muscle IgG1 was inversely correlated with physical performance (400 m walk time:  $r=0.74$ ,  $p=0.005$ ; SPPB score:  $r=-0.73$ ,  $p=0.006$ ) and muscle strength ( $r=-0.6$ ,  $p=0.05$ ). In a murine model, IgG was found to be higher in both muscle and blood of older, versus younger, C57BL/6 mice. Older mice with a higher level of muscle IgG had lower motor activity. IgG in mouse muscle co-localized with cardiac troponin T (cTnT) and markers of complement activation and apoptosis/necroptosis. Skeletal muscle-inducible

**Supplementary Information** The online version contains supplementary material available at <https://doi.org/10.1007/s11357-022-00513-7>.

T. Zhang (✉) · J. Dong · Z. Xu · B. Feng · B. Nicklas · S. Kritchevsky  
Department of Internal Medicine, Section On Gerontology and Geriatric Medicine, Wake Forest School of Medicine, Winston-Salem, NC 27157, USA  
e-mail: tzhang@wakehealth.edu

T. Zhang · B. Nicklas · S. Kritchevsky  
Sticht Center for Healthy Aging and Alzheimer's Prevention, Wake Forest School of Medicine, Winston-Salem, NC, USA

X. Feng  
Department of Otolaryngology, Wake Forest School of Medicine, Winston-Salem, NC, USA

*Present Address:*  
Z. Xu  
Department of Geriatrics, First Affiliated Hospital, Zhejiang University School of Medicine, Hangzhou, China

*Present Address:*  
B. Feng  
Department of Geriatrics, Guang'Anmen Hospital, Beijing, China

K. M. Haas  
Department of Microbiology and Immunology, Wake Forest School of Medicine, Winston-Salem, NC, USA

P. M. Cawthon  
Resarch Institute, California Pacific Medical Center and Department of Epidemiology and Biostatistics, University of California, San Francisco, CA, USA

K. M. Beavers  
Department of Health and Exercise Science, Wake Forest University, Winston-Salem, NC, USA

cTnT knockin mice also showed elevated IgG in muscle and an accelerated muscle degeneration and motor activity decline with age. Most importantly, anti-cTnT autoantibodies were detected in the blood of cTnT knockin mice, old mice, and older humans. Our findings suggest a novel cTnT-mediated autoimmune response may be an indicator of sarcopenia.

**Keywords** Sarcopenia · Cardiac troponin T · Autoimmunity · Older adults · Mice · Transgenic mice

## Introduction

Age-related muscle mass and strength decline (sarcopenia) impairs the performance of daily living activities and can lead to debilitating declines in function. These are major contributors to morbidity and mortality in older adults, leading to decreased quality of life and increased health care costs [1, 2]. Currently, there are no accepted blood-based biomarkers of sarcopenia. Novel biomarkers can help increase our understanding of the mechanisms underlying decreased muscle mass and strength with age to drive intervention development.

Autoimmunity plays a critical role in several muscular diseases [3–7] and immunoglobulin G (IgG) deposition/infiltration within skeletal muscle fiber has been found in some muscle diseases in rodents, non-human primates, and humans [3–5, 7–16]. In some of these diseases, IgG targets key neuromuscular junction (NMJ) molecules and membrane receptors (e.g., muscle-specific kinase, acetylcholine receptor, and ryanodine receptor) and leads to impaired muscle innervation and muscle fiber membrane abnormalities [6, 9, 11, 12, 17–21]. In other mouse muscle disease models (e.g., Duchenne muscular dystrophy [22] and dysferlin-deficient mouse [23]) and in aged mice [24], IgG infiltration in fiber has been recognized as a marker of increased fiber membrane permeability. In recent studies of Duchenne muscular dystrophy patients and mouse models, IgG was co-localized with necroptosis markers and macrophage markers [25], indicating a potential association of IgG with autoimmune-related muscle fiber damage [26].

Autoimmunity increases with age [27, 28] with some studies finding that circulating IgG also increases with age in humans [29–32]. This

age-dependent increase of IgG in human serum occurs in an IgG subclass-specific manner, with IgG1 increasing in both men and women [30]. A genome-wide association study of 256,523 older adults (60 years and older) showed that HLA-DQ alleles involved in autoimmune disease were strongly associated with muscle weakness [33]. Taken together, the literature raises the possibility that IgG may play a novel role in sarcopenia, potentially through an autoimmune response. However, important gaps in our understanding of the role of autoimmunity in sarcopenia remain and the autoantigens in the skeletal muscle still need to be determined.

Skeletal muscle expressed cardiac troponin T (cTnT) may be an antigen relevant to sarcopenia development. TnT is a key component of contractile machinery essential for muscle contraction [34]. There are three expressed TnT isoforms. These isoforms are present in slow skeletal muscle (TnT1), fast skeletal muscle (TnT3), and cardiac muscle (cTnT). However, cTnT can be expressed in skeletal muscle under certain conditions (e.g., after sciatic nerve denervation [35, 36]) and in certain neuromuscular diseases [37, 38]. In some muscle disorders (e.g., Duchenne muscular dystrophy and dysferlin-deficiency/mutation), where skeletal muscles are known to have elevated IgG deposition/infiltration [23, 25], cTnT mRNA levels were also found to be higher than that in the normal skeletal muscle, as was revealed by human gene microarray data (GSE3307, NCBI GEO dataset [39, 40]). In addition, cTnT mRNA levels in skeletal muscle are higher in older, compared to younger, adults in another cohort study (GSE28422, NCBI GEO dataset) [41], indicating an age-related increase of cTnT expression in human skeletal muscle. This is consistent with our previous report that cTnT expression in skeletal muscle of C57BL/6 mice increases with age and plays a critical role in mediating NMJ denervation in skeletal muscle of old mice [42]. Notably, anti-cTnT autoantibodies have been found in blood from humans with no known muscular pathology [43, 44]. Although cTnT in skeletal muscle increases with age [42], whether skeletal muscle cTnT is targeted by the anti-cTnT autoantibodies that subsequently lead to muscle damage and function decline is still unknown.

We present data intended to bridge some of the above gaps and to elucidate if an autoimmune response plays any role in skeletal muscle aging and,

if so, what underlying autoantigens in the skeletal muscle are targeted. Our results, for the first time, demonstrate that older adults' skeletal muscle has IgG deposition and its levels are negatively associated with muscle strength and physical performance.

## Materials and methods

### Reagents and antibodies

Monoclonal rabbit anti-human IgG1 (SA5-10,202), IgG2 (SA5-10,203), IgG3 (SA5-10,204), and IgG4 (SA5-102,025) recombinant antibodies are from ThermoFisher Scientific (Carlsbad, CA). Rabbit anti-Mouse IgG antibodies IgG470 (ab133470) and IgG475 (ab190475), human IgG-specific antibody IgG489 (ab109489), anti-CD68 antibody (ab125212), and anti-Dystrophin antibody (ab15277) are from Abcam (San Diego, CA). Rabbit anti-PKA R1 $\alpha$  (D54D9) was purchased from Cell Signaling (Danvers, MA). Albumin Antibody (clone 188,835) was purchased from NOVUS (Centennial, CO). Alexa Fluor® 680 AffiniPure Goat Anti-Mouse IgG, Fc $\gamma$  subclass 1 specific (115–625-205), Fc $\gamma$  subclass 2a specific (115–625-206), Fc $\gamma$  subclass 2b specific (115–625-207), Fc $\gamma$  subclass 3 specific (115–625-209), and Alexa Fluor® 680 AffiniPure Fab Fragment Goat Anti-Mouse IgG2c (115–627-188) are from Jackson Immuno Research Laboratories (West Grove, PA). Rabbit anti-cTnT polyclonal antibody (MBS767506) was purchased from MyBioSource (San Diego, CA), and mouse anti-cTnT antibody 4B8 was generated in laboratory of Dr. Jian-Ping Jin (Wayne State University, Detroit, MI, USA), previously shown to be highly specific for cTnT in multiple species without cross-reaction to the fast or slow isoforms of TnT [45]. Fluorescein-Conjugated Goat IgG Fraction To Mouse Complement C3 (SKU0855500) was purchased from MP Biomedicals (Irvine, CA). Rabbit RIPK3 Antibody (ARP31513\_T100) and rabbit TnT3 antibody (ARP51287\_T100) are from AVIVA Systems Biology (San Diego, CA). Rabbit caspase-3 Antibody #9662 and caspase-9 Antibody #9504 were from Cell Signaling (Danvers, MA). Rabbit TnT1 antibody (GTX109585) was purchased from Genetex (Irvine, CA). Rabbit anti-Flag antibody (PA1-984B and 740,001) was from ThermoFisher Scientific. GAPDH antibody (AM4300); Alexa Fluor

594-conjugated Wheat Germ Agglutinin (WGA, W11262); Alexa Fluor 488-, 594-, or 647-conjugated  $\alpha$ -Bungarotoxin; and Alexa Fluor 488-, 680-, or 790-conjugated Goat anti-mouse and anti-rabbit IgG were all purchased from ThermoFisher Scientific. CF™680-conjugated goat-anti-human IgG (SAB4600363) was purchased from Sigma-Aldrich (St. Louis, MO). VECTASHIELD HardSet Antifade Mounting Medium with DAPI was from Vector Laboratories (Burlingame, CA).

### Human study participants

Frozen muscle tissue collected from participants who were previously enrolled in two different clinical studies were used for this study. All participants were non-smoking, not on hormone replacement therapy, sedentary (<15 min of exercise, 2 times/week), and weight stable (<5% weight change) for at least 6 months prior to enrollment and the skeletal muscle biopsy. All had normal liver, kidney, pulmonary, and thyroid function; no history of excessive alcohol intake; and no major chronic illness, anemia, or orthopedic impairment as described [46]. Specifically, 11 subjects (8 men, 3 women, age:  $68 \pm 4.6$  years; BMI:  $29.3 \pm 2.0$  kg/m<sup>2</sup>) were from the NIH-funded Improving Muscle for Functional Independence Trial (IMFIT, NCT01049698) [47]), while another 12 (2 men, 10 women, age:  $67 \pm 4.5$  years; BMI:  $33.8 \pm 4.9$  kg/m<sup>2</sup>) were participants in the SILVER study (NCT01298817) [48]. Both studies were approved by the Wake Forest Institutional Review Board and all participants signed informed consent to participate in the study.

### Human skeletal muscle biopsy and plasma collection

Needle biopsies of the vastus lateralis were collected at baseline, prior to either study intervention, under local anesthesia with 1% lidocaine. All biopsies were performed in the early morning after an overnight fast. Subjects were asked to refrain from taking aspirin, prescription, and over-the-counter non-steroidal anti-inflammatory drugs, or other compounds that may affect bleeding, platelets, or bruising for the week prior to the biopsy, and to refrain from any strenuous activity for at least 36 h prior to the biopsy. Visible blood and connective tissue were removed from the muscle specimen. A muscle portion (30 mg)

used for RNA and protein extraction was snap-frozen in liquid nitrogen under RNase-free conditions, and stored at  $-80^{\circ}\text{C}$  until analysis. Another portion with similar size was embedded in tissue-freezing medium (ThermoFisher Scientific, Carlsbad, CA), frozen in liquid nitrogen, and then stored at  $-80^{\circ}\text{C}$  until sectioning. Whole blood from participants was collected in sodium EDTA tubes before muscle collection. Centrifugation was then performed at  $4^{\circ}\text{C}$  with an initial spin at 2000 g for 10 min to separate the plasma from the buffy coat and red blood cells and was stored at  $-80^{\circ}\text{C}$  until analysis.

#### Physical function, mobility, and knee extensor strength

Mobility was measured by using a 400-m walk test for time. The participants were instructed to complete the distance (10 laps on a flat indoor surface 20 m in length) as quickly as possible without running [47]. Lower-extremity function was assessed with the Short Physical Performance Battery (SPPB) [49], which consisted of a standing balance test, usual gait speed over a 4-m course, and time to complete 5 repeated chair rises with arms folded across the chest. Results from each of the 3 tests were scored from 0 (inability to perform the task) to 4 and summed for the total SPPB score, which ranged from 0 (lowest function) to 12 (highest function). Maximal isokinetic knee extensor strength was assessed using an isokinetic dynamometer (Biodex) at a fixed speed ( $60^{\circ}$  per second) with the participant sitting and the hips and knee flexed at  $90^{\circ}$ . This method is widely considered the gold standard of strength assessment [50]. The 1-week test–retest reliability in our lab is very high (intra-class correlation coefficient  $>0.97$ ). We used the peak torque observed during this range of motion as the measure of strength for each knee extension movement.

#### Mice

Animal housing and procedures were approved by the Animal Care and Use Committee of Wake Forest University Health Sciences. Young and old C57BL/6 mice (2–4 and 20–22 months old, respectively) were purchased from NIA and some of the old mice were maintained in our animal facilities until they reached very old age (26–28 months). We have previously

determined that cTnT isoform g (NP\_001123647) is the major isoform of cTnT elevated with aging in the mouse skeletal muscle by immunoprecipitation and mass spectrometry [42]. To further determine the causal relationship between cTnT and muscle structure and function, we generated the inducible skeletal muscle-specific cTnT knockin (ismcTnT-KI) mice by crossing human  $\alpha$ -skeletal actin (HSA) promoter-driven Cre mice (ACTA1-cre/Esr1, Stock No: 025750 from Jackson Laboratory) with conditional cTnT knockin mice (cTnT-KI, generated by Cyagen). The specificity of this skeletal muscle  $\alpha$ -actin (ACTA1) promoter-driven Cre transgenic mouse has been demonstrated by another lab [51]. For cTnT-KI mice, the “CAG-loxP-Stop-loxP-kozaq-mouse Tnnt2 CDS (NM\_001130175.2, encoding cTnT protein isoform g, without stop codon)-3xFLAG-polyA” cassette was cloned into intron 1 of ROSA26 by CRISPR/Cas-mediated genome engineering. To generate ismcTnT-KI mice, cTnT-KI mice were bred together with ACTA1-Cre/Esr1 mice [51] to yield homozygous cTnT-KI mice either with (Cre-cTnT-KI) or without (cTnT-KI controls) ACTA1-Cre. To induce Cre-mediated knockin of cTnT-3xFLAG allele in skeletal muscles, 20 mg/ml tamoxifen (Sigma, T5648) stock solution in coin oil (Sigma, C8267) was intraperitoneally administered (75 mg/kg/day) [52, 53] for 5 consecutive days for the 2-month-old ismcTnT-KI mice to activate Cre recombinase, which in turn led to cTnT-3xFLAG knockin overexpression exclusively in skeletal muscle cells. The wild-type siblings were used as matched controls that were injected with tamoxifen but where no recombination occurred due to the lack of the Cre recombinase.

#### Genotyping of Cre-cTnT-KI and cTnT-KI mice

Genotyping for cTnT-KI mice was performed from genomic DNA extracted from 21-day-old mouse tail, approximately 3 mm (up to 5 mm), using KAPA Mouse Genotyping Kit (KR0385–v3.16) followed by PCR. LongAmp® Taq DNA Polymerase-M0323L (New England Biolabs, Ipswich, MA) and GoTaq® Master Mixes M7122 (Promega, Madison, WI) were used for PCR reactions. Specifically, PCR primers with the following oligos 5'-CACTTGCTCTCCCAAAGTCGCTC-3', 5'-ATACTCCGAGGCGGATCA CAA-3', and 5'-GCATCTGACTTCTGGCTAATA AAG-3' were used to determine conditional cTnT-KI

and wild-type allele. The amplicons generated were 453 bp for the wild-type allele, and 644 bp for the homozygotes with floxed allele, and were visualized by agarose gel electrophoresis. PCR was also used to detect the presence or absence of the Cre allele with oligos 5'-CATATTGGCAGAACGAAAACGC-3' and 5'-CCTGTTTCACTATCCAGGTTACGG-3' for a 413 bp amplicon. The muscle tissue-specific gene deletion was confirmed by additional PCR assay with the following oligos: 5'-GGCAACGTGCTGGTTATTGTG-3', 5'-AGCTTCTTCCTGTTCTCCTCGTA-3', and 5'-AGATCTGCAAGCTAATTCCTGC-3'. The amplicons generated were 1214 and/or 249 bp for the conditional cTnT-KI allele, and 337 bp for the constitutive cTnT-KI allele (after tamoxifen induced Cre recombination).

#### RNA extraction, PCR, and real-time PCR

Total RNA was extracted from muscle tissues using TRIZOL reagent (ThermoFisher Scientific) according to the manufacturer's instructions. To quantitatively analyze mRNA expression level, 23.5 ng of total RNA was reverse transcribed into cDNA and amplified with the appropriate primers using a one-step kit (Lo-Rox Bio-78005 Biotline) and a thermo cycler (7500 Fast real-time PCR system, Applied Biosystems) for real-time RT-PCR quantitation. Analysis was performed by the comparative threshold cycle (Ct) method under the following cycling conditions: 30 min at 45 °C, 5 min at 95 °C, 40 cycles of 10 s at 95 °C, and 1 min at 60 °C. Relative abundance of each mRNA was determined from the Ct values using the  $2^{-\Delta\Delta C_t}$  method [54] after normalization to GAPDH. All experiments were performed in triplicate. TaqMan probe-based primers (ThermoFisher Scientific) were used in all reactions. Accession numbers are listed following each gene: Mouse *Tnnt2*, Mm01290256\_m1; *chrng*, Mm00437419\_m1; *Runx1*, Mm01213404\_m1; *GAPDH*, Mm03302249\_g1.

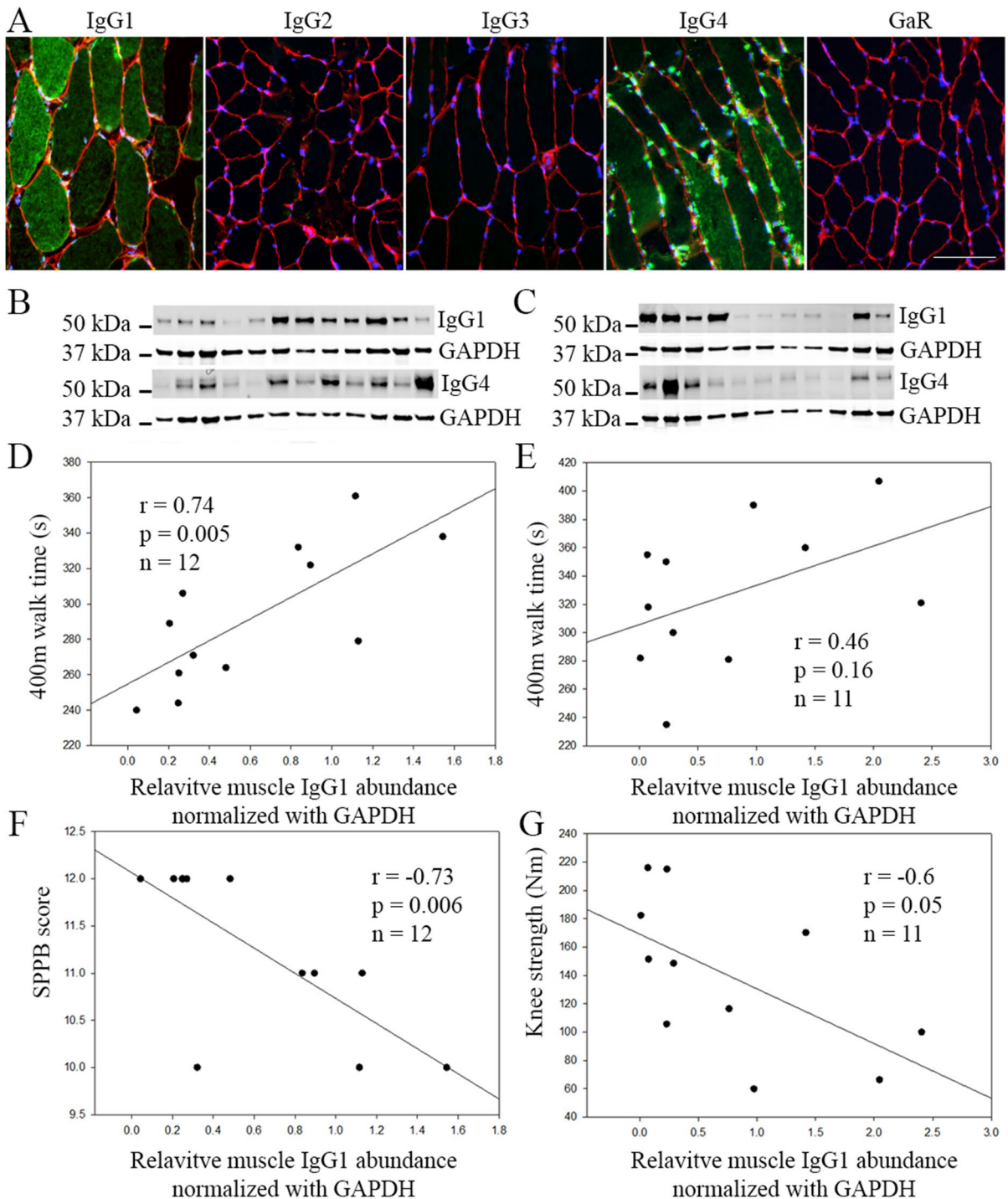
#### Protein extraction, electrophoresis, and immunoblotting

For immunoblotting, muscles were homogenized using a bead blender (BBX24B Bullet Blue Blender, Next Advance) in Eppendorf tubes containing stainless steel beads (0.9–2.0 mm, Next Advance) and 2×Laemmli Sample Buffer (1,610,737, Bio-Rad),

and then cleared by centrifugation as described previously [42, 55]. Protein concentrations were determined using a Bio-Rad DC protein assay kit (Hercules, CA, USA). SDS-PAGE was conducted using MINI-PROTEAN TGX, 4–20% gradient gels from Bio-Rad. Gels were transferred to nitrocellulose membranes (Amersham Health, Little Chalfont, Buckinghamshire, UK) at 4 °C overnight. Blots were blocked in 5% nonfat dry milk with 0.1% Tween-20 in TBS for primary antibody incubation. Specific proteins were detected with individual primary antibodies at 4 °C overnight, and Alexa 680-conjugated secondary antibodies were used at a 1:10,000 dilution at room temperature for 1 h. Band intensity was measured using an Odyssey imaging system (LI-COR Biotechnology, Cambridge, UK). Data are representative of three independent experiments. Western blot densitometry was carried out using Image J software (National Institutes of Health, Bethesda, MD, USA).

#### Hematoxylin and eosin staining, immunofluorescence staining, and microscopy

Inverted Tissue Culture Microscope with 1.3MP USB Camera (SKU: IN200TA-M) and AmScope software were used to collect the color hematoxylin and eosin (H&E) staining image. For immunofluorescent staining, 12- $\mu$ m cross-sectional cryosections from human or mouse muscles were mounted onto glass slides, which were fixed with 2% PFA in PBS for 10 min and permeabilized with 0.5% Triton X-100 in PBS for 5 min at room temperature. After three washes with PBS, they were incubated for 1 h in blocking buffer (PBS with 10% normal goat serum (Vector Labs, Burlingame, CA)), and labeled with primary and secondary antibodies overnight at 4 °C and 1 h at room temperature in a wet box, respectively. To allow the even staining of tissue, the blocking buffer and diluted primary and secondary antibodies were all covered with a piece of parafilm during incubation for even distribution of antibodies. Alexa Fluor 594- or 647-conjugated  $\alpha$ -bungarotoxin were incubated together with the secondary antibody. They were then mounted in HardSet Antifade Mounting Medium with DAPI (H-1500, Vector Lab). Wide-field immunofluorescence images were taken on an inverted motorized fluorescent microscope (Olympus, IX81, Tokyo, Japan) and an Orca-R2 Hamamatsu CCD camera



(Hamamatsu, Japan). The camera driver and image acquisition were controlled with a MetaMorph

Imaging System (Olympus) under the same parameters for each sample on the same slide. Digital

◀**Fig. 1** Protein levels of skeletal muscle IgG1 but not IgG4 are negatively associated with muscle strength and physical performance. (A) Representative immunofluorescence staining image of different IgG subclasses in vastus lateralis skeletal muscle fibers of older adults. Unconjugated Rabbit anti-Human IgG1, 2, 3, and 4 antibodies were used as primary antibodies, and Alexa488 conjugated Goat-anti-Rabbit secondary antibody (GaR) was used to detect IgG subclasses (green) in the muscle. Alexa Fluor 488-conjugated GaR alone was used as a negative staining control. Fiber membrane was stained with Alexa Fluor 594-conjugated Wheat Germ Agglutinin in red and nuclei were stained with DAPI in blue. Scale bar, 100  $\mu$ m. Immunoblot of IgG1 and IgG4 in the limb muscle of 12 SILVER study subjects (B) and 11 IM FIT study subjects (C). GAPDH was used as an internal loading control. (D) Pearson correlation assay revealed a positive correlation between IgG1 and 400 m walk time in SILVER subjects. A similar trend observed in IMFIT subjects (E). IgG1 is negatively correlated with SPPB score in SILVER subjects (F) and with knee extensor strength in IMFIT subjects (G)

image files were transferred to Photoshop 7.0 to assemble montages.

Circulating autoantibody screening by immunoblot or dot blot

Recombinant proteins used for immunoblot and dot blot were either custom ordered or purchased from companies. Mouse TnT3 isoform 8 protein with a fusion His-SUMO (Small Ubiquitin-like Modifier) tag and SUMO tag control protein were from GenScript. Human cTnT isoform 11 protein ab86685 was purchased from Abcam, NBP2-61,383 was from NOVUS, and J34510 from BiosPacific, the same one used in the literature for circulating cTnT autoantibody detection in human blood [44]. Recombinant human TnT3 protein MBS2011217 was purchased from MyBiosource, and recombinant human TnT1 protein GTX109585 was from GeneTex. For immunoblot, 20 ng recombinant protein denatured in 10  $\mu$ l 2 $\times$ Laemmli Sample Buffer was load each lane. For dot blot, 20–100 ng native recombinant protein (2–10  $\mu$ l) was loaded directly onto nitrocellulose membrane (Amersham Health, Little Chalfont, Buckinghamshire, UK) and incubated 1 h at room temperature until the membrane was dry. The rest of the steps just followed regular immunoblotting procedures, except that pooled serum or plasma from mice or older adults (1:100–500 dilution) was used as primary antibodies. For dot blot assay with antigen blocking, the pooled plasma (300  $\mu$ l) was firstly

incubated with 0.5 ml 5% non-fat milk/TBST with or without an overdose (100 ng/ $\mu$ l  $\times$  10  $\mu$ l) of recombinant cTnT protein (J34510, BiosPacific) for 30 min at room temperature. An additional 4 ml 5% milk/TBST was further added to each plasma mix with or without antigen blocking. Then both of them were further used for immunoblotting assay of two identical NC membrane samples loaded with the same 200 ng recombinant cTnT protein.

#### Wire hang test

Motor activity was evaluated by using a Wire Hanging Test which is indicator of abdominal and limb muscle fatigability [25, 56]. Briefly, mice were placed on a grid which was then gently inverted so that mice were hanging under the grid. The latency to fall was recorded and normalized to the body weight of each mouse, cage top, which were then inverted and suspended above the home cage. Two measurements were performed per mouse and the maximum hanging time (in seconds) was used for statistical evaluation. These experiments were conducted in a blinded fashion.

#### Statistical analysis

Data analysis was performed with SigmaPlot 11.0 (Systat Software, San José, CA) and Prism 7.0 (Graphpad, La Jolla, CA). All data are presented as means  $\pm$  SEM. An  $\alpha$ -value of  $P < 0.05$  was considered significant. The Pearson Product Moment Correlation was used to measure the strength of the association between pairs of variables.

## Results

Skeletal muscle IgG1 is negatively associated with physical function in older adults. There are 4 human IgG subclasses (IgG1, IgG2, IgG3, and IgG4). Using immunofluorescence staining, we found that IgG1 and IgG4 are the predominant IgG subclasses localizing in some muscle fibers of older adults. In contrast, IgG2 and IgG3 were barely detectable in the muscle of older adults (Fig. 1A). Consistently, immunoblotting detected mainly IgG1 and IgG4 protein expression in the skeletal muscle of old adults (Fig. 1B, C), with IgG2 and IgG3 barely detected (data not shown).

The relative abundance of IgG1 and IgG4 in the skeletal muscle was further determined by normalization with GAPDH in each sample and quantitation with ImageJ. The association between the GAPDH normalized relative abundance of skeletal muscle IgG1, IgG4, or IgG1 and IgG4 combined and physical function, mobility, and knee extensor strength was then analyzed. Strikingly, in SILVER study participants, IgG1 protein levels in skeletal muscle showed a strong negative correlation with SPPB score ( $r = -0.73$ ,  $p = 0.006$ ) and a positive correlation with 400 m walk time ( $r = 0.74$ ,  $p = 0.005$ ) (Fig. 1D, E). When expressed in seconds to complete the 400 m walk, each SD increment in IgG1 protein relative abundance is associated with a 29-s-longer 400-m walk time, or each SD increment in IgG1 protein was associated with a  $-0.13$  m/s slower walking speed. Similarly, in IMFIT study participants, IgG1 protein levels in skeletal muscle showed a positive correlation with 400-m walk time that did not reach statistical significance ( $r = 0.46$ ,  $p = 0.16$ ) and a negative correlation with knee extensor strength ( $r = -0.60$ ,  $p = 0.05$ ) (Fig. 1F, G). Notably, a significant difference in the knee extensor strength was observed between the IgG1 low and IgG1 high groups (Supplementary Fig. 1). In contrast, skeletal muscle IgG4, or IgG1 and IgG4 combined, did not show any significant correlation with physical function, mobility, and knee extensor strength in IMFIT or SILVER study subjects (data not shown).

IgG level increases with age in skeletal muscle of C57BL/6 mice and is associated with muscle functional and structural abnormality in the aged mice. To better understand the implications of our human findings, we used a murine model to understand age-related and mechanistic questions. We examined IgG protein levels in the skeletal muscle of young, old, and very old C57BL/6 mice. We found that IgG protein levels increase with age in both skeletal muscle and in blood (Fig. 2A, B). In addition, mice with higher level of skeletal muscle IgG deposition demonstrated a lower level of motor activity compared to the mice with lower or no skeletal muscle IgG deposition (Fig. 2C, D), a finding similar to that observed in older adults (Supplementary Fig. 1). By immunofluorescence staining, the subcellular localization of IgG in muscle was found to be mainly at neuromuscular junction (NMJ) or within myofibers of the aged mice and is co-localized with markers of C3

complement activation and necroptosis (RIPK3 [25]), and IgG-infiltrated myofibers also showed reduced level of dystrophin on the fiber membrane (Fig. 3). Interestingly, the IgG infiltration/deposition in muscle of aged mice is also subclass specific, with IgG3 subclass mainly found at the NMJ while IgG2b and IgG2c mainly in myofibers and interstitial area of old and very old mice (Supplementary Fig. 2).

cTnT could be one of the autoantigens that are targeted by IgG autoantibodies in the skeletal muscle of aged mice. We have previously reported that cTnT in skeletal muscle of old mice increases with aging and is enriched at NMJ of aged mice muscle [57]. In this study, we further found that cTnT was co-stained with IgG (Fig. 4(A)), which was found to co-localize with C3 complement, and the markers of necroptosis in the skeletal muscle of aged mice (Fig. 3). Markers of activated apoptosis (caspase-3 or caspase-9) were also detected at cTnT and IgG positive areas, mainly at the NMJ area in aged mice (Supplementary Fig. 3). Given that cTnT autoantibodies have previously been found in human blood [44], the co-presence cTnT and IgG in the skeletal muscle indicated a potential autoimmune response in the muscle. To determine if there are anti-cTnT autoantibodies in the blood of the aged mice, we performed an immunoblot assay using various recombinant TnT proteins as antigens to screen their respective autoantibodies in the serum of young and aged mice. We found that recombinant cTnT protein was detected by the anti-serum from aged mice or by a rabbit anti-cTnT antibody (MBS767506), but not by anti-serum from young mice (Fig. 4(B)), indicating the presence of anti-cTnT autoantibodies in the blood of aged mice. In contrast, recombinant mouse TnT1 or TnT3 proteins were not detected by the serum of aged mice, although TnT1- and TnT3-specific antibodies detected their respective recombinant TnT proteins and endogenous TnT isoforms in the mouse muscle with high specificity (Supplementary Fig. 4).

Newly generated tamoxifen-inducible skeletal muscle-specific cTnT knockin (ismcTnT-KI) mice showed an impact of cTnT overexpression on muscle structure and function. We have previously determined that cTnT isoform g (NP\_001123647) is the major isoform of cTnT elevated with aging in the mouse skeletal muscle [57]. Given our detection of anti-cTnT autoantibodies in the serum of aged but not young mice, and co-localization of IgG, cTnT, and



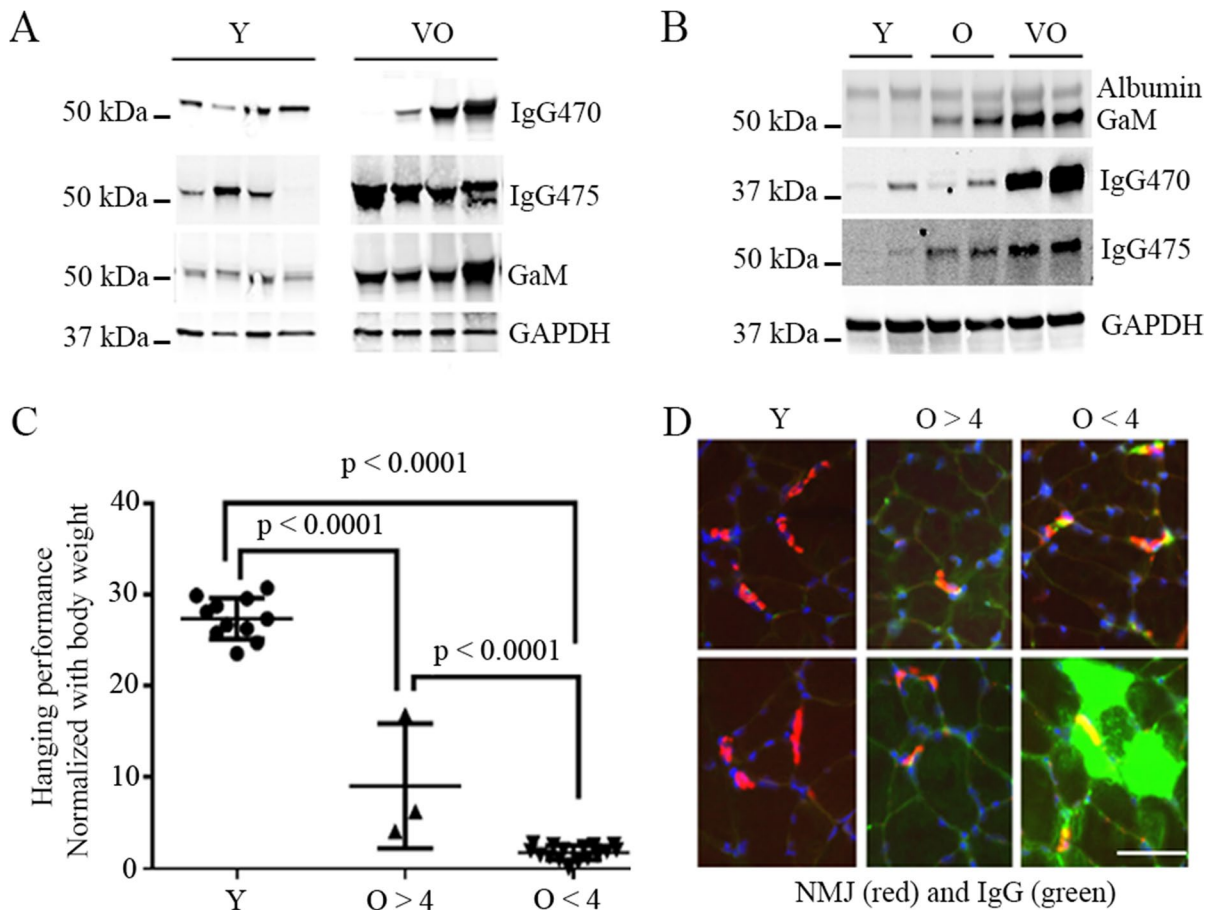


**Fig. 2** IgG levels in blood and in skeletal muscle increases with age in C57BL/6 mice and mice with lowest level of motor activity had highest level of muscle IgG deposition at NMJ or within myofiber. **(A)** Blood total IgG detected by immunoblot with mouse IgG-specific antibody IgG470 (ab133470) and IgG475 (ab190475), respectively. **(B)** Tibialis anterior muscle total IgG detected by immunoblot with ab133470 and ab190475. Data is representative of 11 young (Y) and 19 old (O, 20–22 months) and very old (VO, 26–28 months) mice. Albumin was evenly detected among young and old mice skeletal muscles. GAPDH was used as internal loading control in both blood and muscle. Goat-anti-mouse IgG? antibody (GaM) alone also detected IgG protein in both blood and muscle.

**(C)** Wire hanging performance (expressed in ratio: maximum hanging time in seconds/body weight in gram) comparison. Mice are with mixed sex with 11 young mice and two groups of old mice grouped based on ratio: O > 4 (old and very old mice with wire hanging performance ratio > 4, 22 months,  $n=1$ ; 27 months,  $n=2$ ) or O < 4 (old and very old mice with wire hanging performance ratio < 4, 22 months,  $n=3$ ; 27 months,  $n=13$ ). **(D)** Representative IgG immunofluorescence staining patterns in tibialis anterior muscles of mice examined in **(C)**. IgG infiltration or deposition (green) in muscle is mainly enriched at NMJ (11 out of 16) (red, stained with Alexa Fluor 594-conjugated  $\alpha$ -bungarotoxin) or within myofibers (10 out of 16) of old and very old mice. Scale bar, 50  $\mu$ m

other markers of complement activation or apoptosis/necroptosis within skeletal muscle of aged mice, we hypothesized that overexpressed cTnT in the skeletal muscle may cause muscle degeneration and function decline through activation of autoimmune response. To test this with highly specific cTnT overexpression in skeletal muscle of the mice, we have generated tamoxifen-inducible skeletal muscle cTnT

knockin mice (ismcTnT-KI) by crossing skeletal muscle  $\alpha$ -actin promoter-driven Cre transgenic mice [51] with conditional cTnT knockin mice (cTnT-KI) (generated by Cyagen, see construction and genotyping details in the “Materials and methods” section). All mice are in C57BL/6 background and were genotype confirmed with PCR following Cyagen protocols (data not shown). After 14 days of cTnT

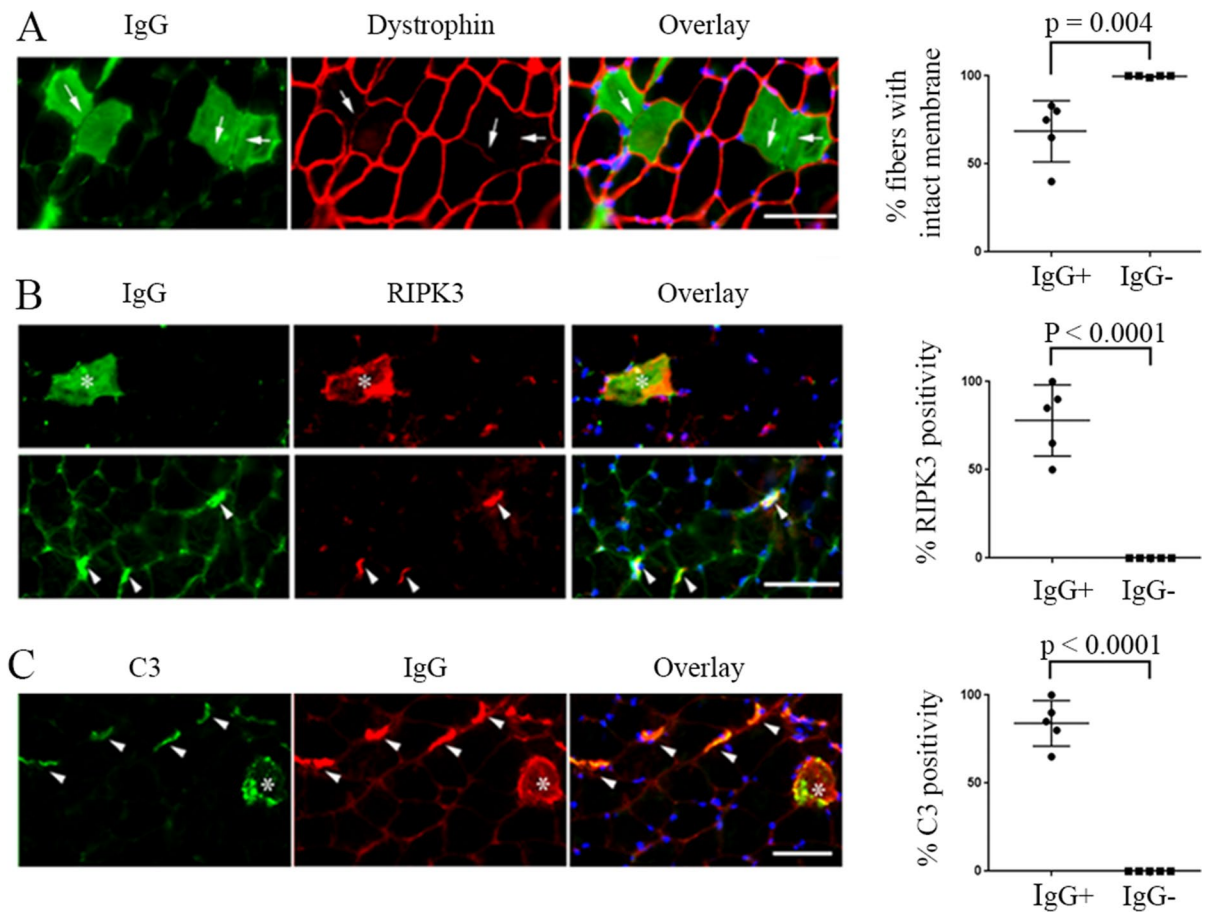


**Fig. 3** IgG in skeletal muscle of aged mice are associated with decreased myofiber membrane integrity and increased necroptosis, and complement activation. **(A)** IgG-infiltrated myofibers have less membrane integrity as revealed by reduced level or absence of membrane dystrophin (arrows). **(B)** IgG-enriched myofibers (asterisks) and NMJs (arrow-

heads) have elevated RIPK3, a marker of necroptosis. **(C)** IgG deposition within fibers (asterisks) and at NMJ (arrowheads) are co-localized with activated C3 complement. Immunofluorescence staining images are representative of 5 old and very old mice. Scale bars, 50  $\mu$ m

overexpression in 2–3-month-old young mice, immunoblotting already detected elevated 3 $\times$ Flag tagged cTnT protein overexpression in all skeletal muscles of ismcTnT-KI mice but not in their brain or heart or in the control cTnT-KI mice treated also with tamoxifen (Fig. 5A). This data confirmed the highly specific knockin cTnT overexpression is highly specific to all skeletal muscles in the ismcTnT-KI mice. To further determine the age-dependent effects of cTnT overexpression on skeletal muscle structure and function, we next monitored their motor activity changes monthly after tamoxifen treatment for a total of 4 months and compared between ismcTnT-KI and control cTnT-KI mice. Strikingly, in great contrast to the control

cTnT-KI mice that showed age-dependent increase in motor activity, all ismcTnT-KI mice showed accelerated decline in motor activity despite both groups tested were at a similar adulthood age, which was about 4–8 months during their tests (Fig. 5B, C). Here we used percent changes in motor activity analysis for each individual mouse since it is known that there exists wide variation in physical performance within each age group (young, old, and very old) in C57BL/6 mice [58]. Importantly, compared to age-matched control cTnT-KI mice, these ismcTnT-KI mice showed increased level of muscle degeneration [59] (e.g., smaller fibers with irregular outline shape, vacuoles, and fiber lesions) (Fig. 6A, F). The knockin

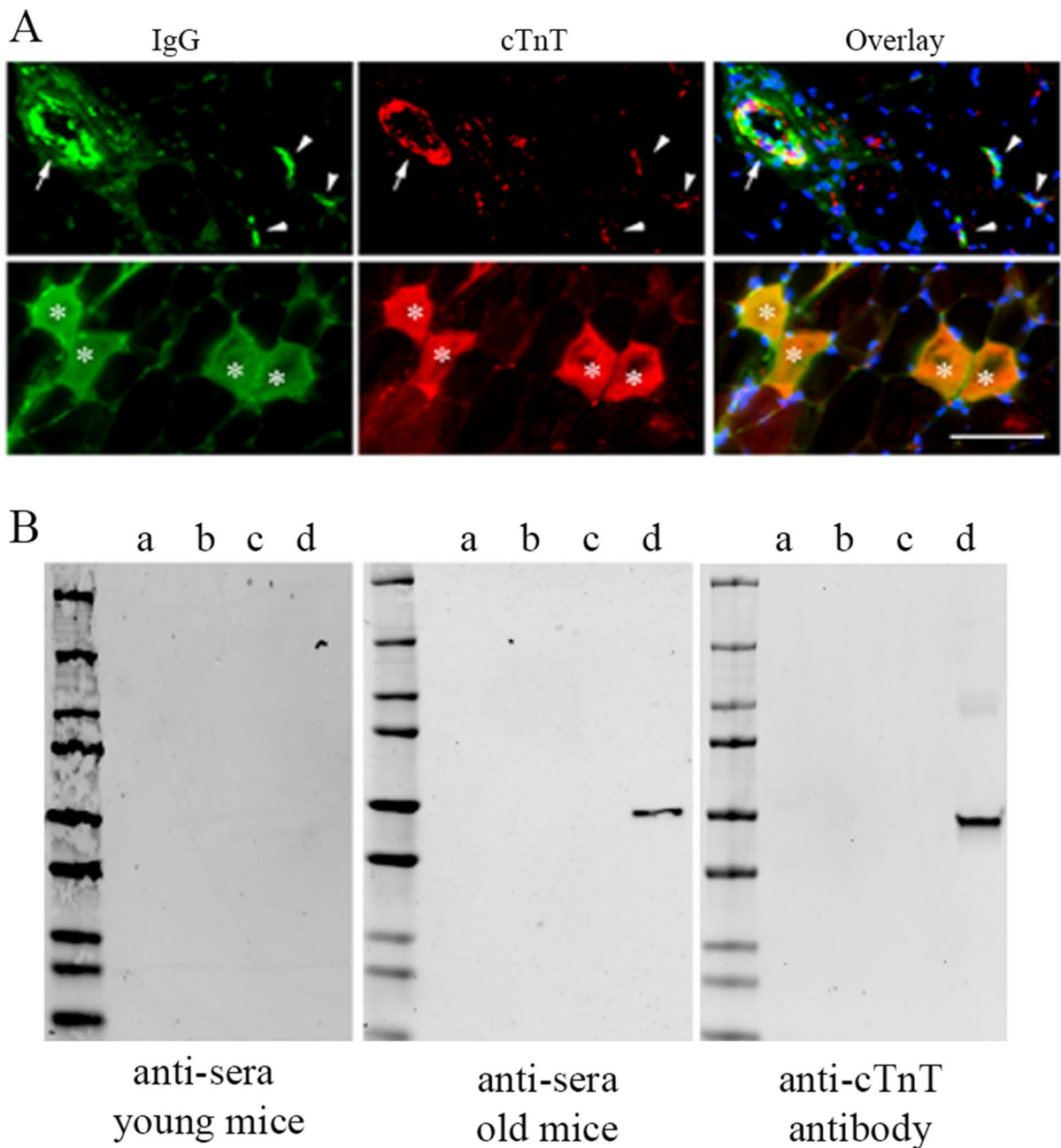


**Fig. 4** IgG anti-cTnT autoantibodies may target cTnT in the skeletal muscle of old mice. (A) Representative immunofluorescence staining image showing co-localization of IgG (stained with Alexa Fluor-488 conjugated Goat-anti-Mouse IgG) and cTnT (stained with MBS767506 and Alexa Fluor-568 conjugated Goat-anti-Rabbit) in skeletal muscle of old mice within myofibers (asterisks), at NMJs (arrowheads), and along blood vessel wall (arrow). Similar to findings in Fig. 3B and C, all most all IgG positive areas were also positive with cTnT staining. We did Goat-anti-Rabbit secondary antibody alone or with Goat-anti-Mouse secondary antibody, which did not show any signal in red (data not shown). Scale bar, 50  $\mu$ m. (B)

Immunoblot assay using recombinant TnT proteins detected anti-cTnT autoantibodies in serum from old mice. Pooled sera (1:100 dilution) from young or old mice ( $n=3$  in each age group) and anti-cTnT antibody (MBS767506, Mybiosource) were used as anti-sera or primary antibody, respectively. Recombinant cTnT was only detected by the anti-sera from old mice and anti-cTnT antibody, but not anti-sera from young mice. Recombinant proteins used for the immunoblot (20 ng per lane): a, human TnT1 protein (GTX109585-pro, GeneTex); b, mouse TnT3 isoform 8 protein with a fusion His-SUMO (Small Ubiquitin-like Modifier) tag; c, SUMO tag (GenScript); d, human cTnT isoform 11 protein (ab86685, Abcam)

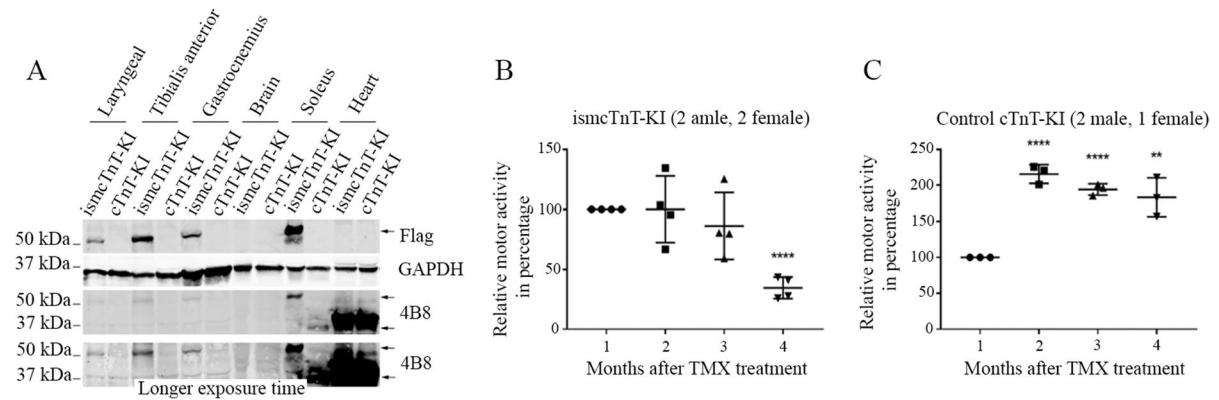


**Fig. 5** Transgenic skeletal muscle cTnT knockin mice showed accelerated motor activity decline with age. **(A)** Representative immunoblot shows that cTnT-3xFlag is only expressed in skeletal muscle, but not in the brain or heart of ismcTnT-KI mice. Both anti-flag and 4B8 (anti-cTnT) antibodies detected the specific cTnT-3xFlag bands. **(B–C)** Motor activity (cage

hanging assay) was measured at 1, 2, 3, and 4 months after the last tamoxifen (TMX) ip injection. Month 1 was set at 100%, and the following months were normalized to month 1 respectively. Both ismcTnT-KI mice **(B)** and control mice **(C)** are about 4–8 months old during the time for test. \*\*\*\* $p < 0.0001$ ; \*\* $p < 0.01$

overexpression in skeletal muscle was confirmed with immunofluorescence staining (Fig. 6B) and the skeletal muscles of ismcTnT-KI mice were found to have increased levels of IgG and complement C3 deposition at NMJ (Fig. 6C) and/or within muscle fibers (data not shown), similar to findings in the muscle of the aged mice. In addition, the NMJs in ismcTnT-KI mice are largely smaller (Fig. 6D, G) with reduced level or absence of PKA-R1 $\alpha$  compared to the control mice (Fig. 6E, H). Level of muscle denervation determined by qRT-PCR of chrng [60, 61] and Runx1 [62, 63] was also found to be higher in ismcTnT-KI mice (Supplementary Fig. 5). CD68 + macrophage infiltration [64] in ismcTnT-KI mice skeletal muscle was also higher than that in the control mice (Supplementary Fig. 6). Importantly, similar to the aged mice, anti-cTnT autoantibodies were detected by immunoblot assay in the serum of these ismcTnT-KI mice, but not the control cTnT-KI mice (data not shown).

**Detection of anti-cTnT and anti-TnT3 autoantibodies in plasma of older adults** The prevalence of circulating anti-cTnT autoantibodies in 467 healthy human subjects (18–72 years of age) was reported to be 9.9% [44]. We also detected anti-cTnT autoantibodies in the pooled plasma of 6 older adults from IMFIT study using dot blot assay with two different recombinant human cTnT proteins as antigen proteins (NBP2-61,383 from NOVUS and J34510 from BiosPacific);

the latter is the same one used in the literature for circulating cTnT autoantibody detection in human blood [44]) (Fig. 7). To confirm the specificity of the detected plasma autoantibodies by the dot blot assay, we further performed antigen blocking. We showed that after incubating the plasma with an overdose of the recombinant cTnT protein (antigen blocking), the plasma failed to detect the specific cTnT dot on the NC membrane (Supplementary Fig. 7). We further found that the recombinant human TnT3 protein (rhTnT3, MBS2011217 from Mybiosource), but not the recombinant human TnT1 protein (rhTnT1, GTX109585 from GeneTex), was also detected by dot blot assay using the pooled plasma of the same 6 older adults as primary antibody (Fig. 7).

## Discussion

In this study, we showed for the first time that autoimmunity in skeletal muscle may play a critical role in age-related mobility decline and muscle structure and function changes, which may be mediated by cTnT. However, it is possible that other skeletal muscle autoantigens are also involved. Our conclusion is supported by the following evidence: (1) IgG1 and IgG4 were found to be deposited in skeletal muscle fibers of older adults, and GAPDH-normalized relative abundance of skeletal muscle IgG1 was found

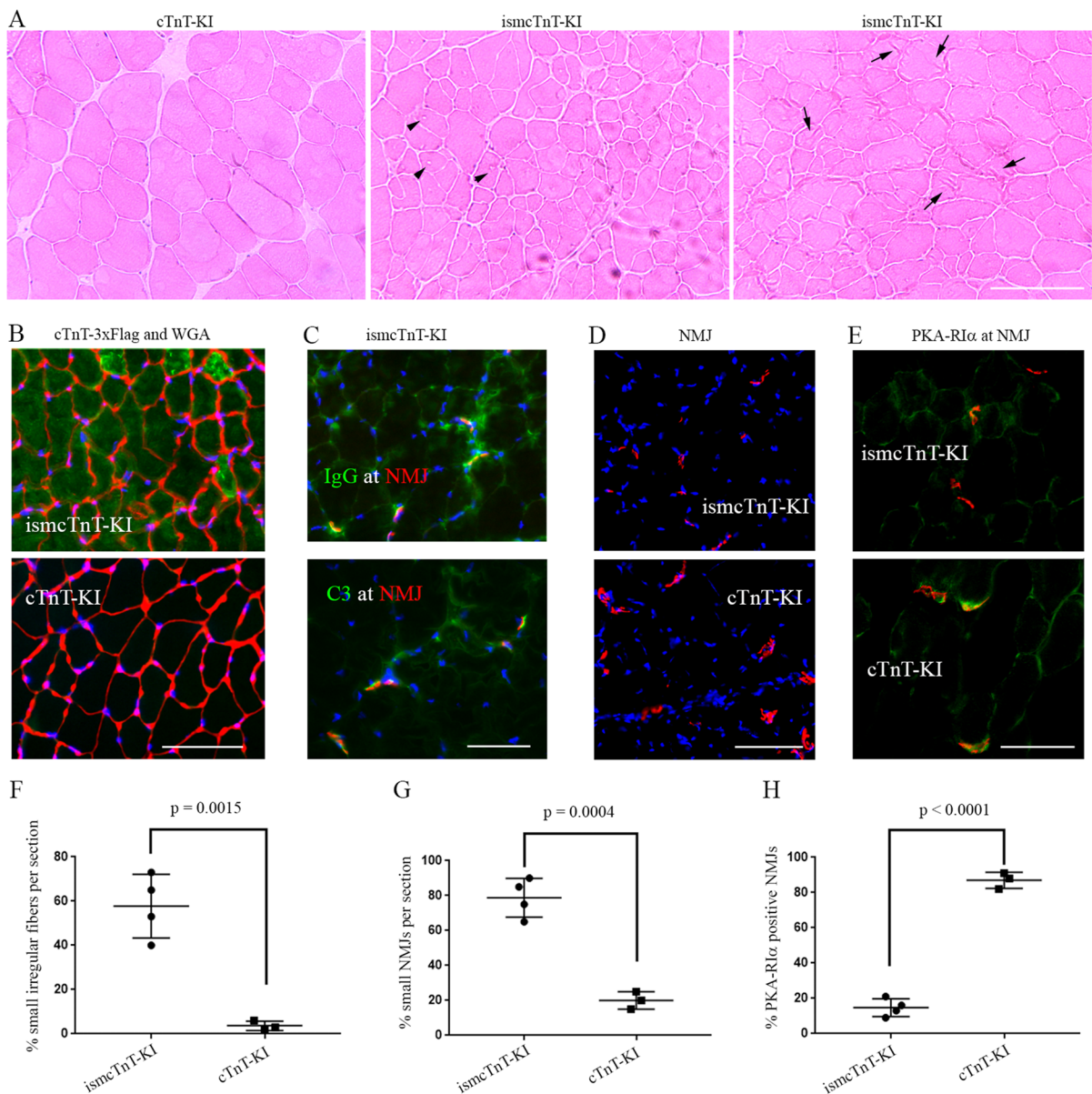


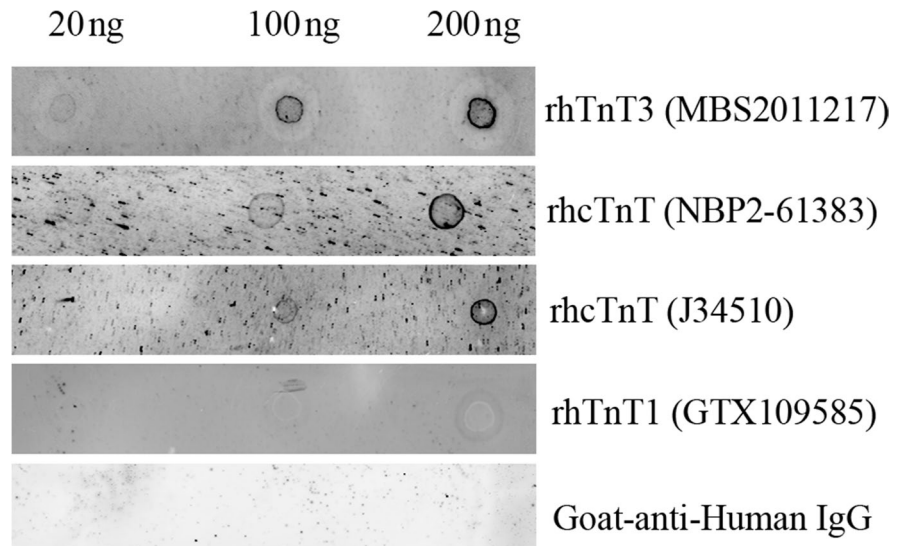
**Fig. 6** Transgenic skeletal muscle cTnT knockin mice showed signs of muscle degeneration and denervation. **(A)** H&E staining of tibialis anterior muscle show ismcTnT-KI mice have many smaller fibers with irregular shape, vacuoles (arrow heads), and lesions (arrows). **(B)** Majority of myofibers in ismcTnT-KI mice have elevated cTnT knockin overexpression (green) with irregular fiber membrane shape labeled in red with WGA (wheat germ agglutinin). **(C)** IgG and C3 (green)

are found at NMJ (red) of ismcTnT-KI mice. **(D)** ismcTnT-KI mice have smaller NMJ size than the control cTnT-KI mice. **(E)** Compared to control cTnT-KI mice, the ismcTnT-KI mice have lower level of PKA-R1 $\alpha$  (green) present at their NMJs (red). Images shown are representative of 4 ismcTnT-KI mice and 3 control mice analyzed. Scale bars, 50  $\mu$ m. **(F–H)** Quantitation of **(A)**, **(D)**, **(E)**, respectively. For PKA-R1 $\alpha$ , at least 20 NMJs were counted in each mouse

to be inversely associated with muscle strength (knee extensor strength) and physical performance (400-m walk time and SPPB, which is highly predictive of future disability and death [49]); (2) IgG

protein levels increased with aging in C57BL/6 mice in both blood and skeletal muscle, and aged (old and very old) mice with a higher level of IgG deposition in skeletal muscle have a lower level of motor

**Fig. 7** Dot blot assay detected cTnT and TnT3 autoantibodies in plasma of older adults. Different amount (20–100 ng) of recombinant TnT3, cTnT, or TnT1 were used for dot blot assay with pooled plasma from 6 IMFIT study subjects as primary antibodies. CF<sup>TM</sup>680 Goat-anti-Human IgG (H+L) was used as secondary antibody only negative control, which failed to detect any recombinant TnT proteins. Elevation of cardiac troponin T



activity, similar to that observed in older adults; (3) IgG positive muscle area in aged mice showed elevated necroptosis/apoptosis, complement activation, and cTnT, with anti-cTnT autoantibodies detected in the blood of aged mice; (4) ismcTnT-KI mice with inducible skeletal muscle cTnT knockin overexpression showed accelerated motor activity decline with age, together with signs of muscle degeneration and denervation, elevated IgG and complement deposition in muscle, and appearance of anti-cTnT autoantibodies in blood; and (5) Both anti-cTnT and anti-TnT3 autoantibodies were detected in the blood of older adults. Although we do not have a younger control group in the human study, based on our findings in young and aged mice, it is highly possible that IgG proteins in younger adults skeletal muscle will be either absent or at a much lower level. In addition, even if we found some IgG in the muscle of younger adults, this will still be expected to fit in to our newly discovered association relationship between muscle IgG levels and the muscle strength or physical function.

#### IgG and complement proteins in skeletal muscle aging

IgG deposition/infiltration in muscle fiber is found in skeletal muscle diseases in rodents, non-human primates, and humans [3–5, 7–16] and is a known marker of increased fiber membrane permeability and damage vulnerability, for instance, in Duchenne

muscular dystrophy [22], dysferlin-deficient myopathy [23], and muscle of aged mice [24]. Apart from age-dependent increase of muscle fiber membrane damage [24] that may lead to increased IgG deposition in muscle, the accumulation of IgG in aged muscle could also have been resulted from increased B cell immunosenescence, which is commonly found in older adults and in centenarians [65] and has been found to be associated with serum IgG levels in the elderly persons [30]. Yet, whether IgG in skeletal muscle increase with age and play a role in age-related muscle damage through immune response activation is still unknown. We showed for the first time that IgG1 and IgG4 are the two main IgG subclasses that are abundantly present in the skeletal muscle fibers of ~50% older adults examined. Data in aging mice model further revealed that IgG levels in the skeletal muscle increase with age and may lead to muscle damage through activation of complement system and cell death pathways. In addition, IgG deposition in skeletal muscle of aged mice is in an IgG subclass specific way, with IgG3 found to be enriched at NMJ while IgG2b, 2c mainly found in muscle fibers. The subclass-specific IgG deposition in muscle strongly indicates that different autoantigens could be targeted by different IgG subclasses in the skeletal muscle. This is supported by previous findings in some muscle disorders. For instance, it is known that human IgG1 is capable of activating the complement system and leads to the post-synaptic membrane damage and reduced number of acetylcholine receptors at

the NMJ, leading to muscle weakness and fatigue [66, 67]. Specifically, in myasthenia gravis (MG), close to 90% of patients have IgG1 antibodies to the acetylcholine receptors. In contrast, approximately 10% of MG patients have MuSK autoantibodies, which are predominantly IgG4 that do not activate complement [68, 69]. We did not see a significant association between muscle IgG4 and muscle strength or function in the older adults; this could be limited by the small sample size in our human study. Although IgG4 binding to its autoantigen does not activate complement system, it could still potentially lead to muscle damage through other well-known autoantibody-induced pathology pathways [70]. For instance, MuSK IgG4 autoantibodies are known to cause MG by inhibiting binding between MuSK and Lrp4 [12, 71]. Future larger cohort studies will help further understand the roles of both IgG1 and IgG4 and determine their respective targeting autoantigens in skeletal muscle of older adults. Our finding that IgG1, but not IgG4, in the skeletal muscle is inversely associated with physical performance and knee extensor strength strongly indicated a possible involvement of complement activation underlying skeletal muscle changes in older adults. Consistently, serum C1q concentration was reported to increase with age, promoting aging-associated decline in skeletal muscle regeneration, and aging-associated impairment of muscle regeneration is restored by C1qa gene disruption [72]. In addition, a recent cross-sectional study identified complement C1q as a potential sarcopenia biomarker, and serum C1q levels were found to be negatively correlated with muscle mass and strength in older adults [73]. Our finding of the co-localization of IgG deposition with C3 in skeletal muscle of aged mice further indicated the involvement of C3 in skeletal muscle aging. C3 plays a central role in complement activation [74], with all three complement activation pathways intersect at the C3 level [75–77]. Complement C3 deficiency has been found to ameliorate aging-related changes in kidney [78] and in hippocampal degeneration [79]. In addition, C3-targeted genetic ablation has been proved to be effective in treating dysferlin-deficient muscle disease in a mouse model [80] and in other age-related structural and functional decline in other tissues, e.g., age-related hippocampal decline [79]. Our finding provided the first evidence that, in addition to C1q, C3 may also be a useful biomarker of sarcopenia and C3 targeting could possibly

be effective in prevention of age-related changes in skeletal muscle. Recent findings also have linked IgG deposition in skeletal muscle to necroptosis [25]. In addition, both caspase-3 and -9 were found to be associated with altered NMJ structure and increased denervation [81, 82]. In addition to cell apoptosis/necroptosis, complement activation also plays a wide range of roles in inflammation, membrane integrity, vascular endothelial cell damage, and metabolism [26, 83–89], all of which are key players in muscle aging. Our findings further suggest that IgG-mediated complement and cell death activation may underlie age-related changes in skeletal muscle.

Mechanisms of autoantibody-induced pathology have been classified into at least 7 categories [70]. Given our findings in aging mice model, the complement activation and subsequent cell lysis induced by apoptosis is one of the most possible pathway that underlies autoimmunity-related sarcopenia. In addition, altered signaling at NMJ or within muscle cells and induction of inflammation could also be involved in this process that mediates autoimmunity-induced muscle damage, which may involve mitochondria oxidative damage [90] and/or skeletal muscle protein degradation. For instance, autoantibodies to acetylcholine receptor on postsynaptic membrane activates complement cascade and leads to membrane attack complex assembly and destruction of postsynaptic membrane protein and structure [91].

TnT and other proteins as skeletal muscle autoantigens in older adults

Although our finding strongly indicates an IgG-mediated activation of complement and cell death pathways underlying skeletal muscle aging, whether an autoimmune response is involved and what are the autoantigens in the skeletal muscle still need to be elucidated. We and others have previously reported a critical role of TnT proteins in regulating apoptosis [92, 93]. The co-localization of IgG with cTnT, complement C3, and markers of apoptosis/necroptosis in the muscle of aged mice, together with detection of anti-cTnT autoantibodies in blood of ismcTnT-KI mice, aged mice, and older humans, strongly suggested that cTnT could be one of the autoantigens that mediate autoimmune response in skeletal muscle sarcopenic changes with age. TnT is a key component of contractile machinery essential for muscle contraction

[34]. There are three TnT isoforms that are expressed in slow skeletal muscle (TnT1), fast skeletal muscle (TnT3), and cardiac muscle (cTnT). Yet, cTnT is also expressed in skeletal muscle under certain conditions (e.g., after sciatic nerve denervation [35, 36]) and in certain neuromuscular diseases [37, 38]. We previously reported that cTnT expression in skeletal muscle of C57BL/6 mice increases with age and, as a known A-kinase anchoring protein [94], plays a critical role in mediating NMJ denervation in fast skeletal muscle of old mice through reducing protein kinase A regulatory subunit RI $\alpha$  (PKA-RI $\alpha$ ) relative abundance at NMJ [42]. Our finding in this study further revealed that in the skeletal muscle of old mice, cTnT could possibly be targeted by its IgG autoantibodies. The consequently activated immune response and complement system may lead to apoptosis and necroptosis at the NMJ or within muscle fibers. Similar to other autoimmune muscle diseases (e.g., MG) where skeletal muscle protein-specific autoantibodies were detected in circulation in the patients, anti-cTnT autoantibodies were also detected in the serum of aged mice, but not in the young mice. Using our newly generated inducible skeletal muscle-specific cTnT knockin mice model, we have further confirmed that anti-cTnT autoantibodies are present in the serum of these transgenic mice, with increased muscle IgG and complement deposition, increased muscle degeneration/denervation, macrophage infiltration, and accelerated motor activity decline with age in adulthood mice. In mice, muscle mass and force production slowly decreases from adulthood (6–9 months of age) to old age (22–24 months), with a rapid deterioration present once mice reach oldest-old ages, geriatric stage (> 26–28 months) [58, 95–97]. Mice at the adulthood age (6–9 months) usually do not have any apparent age-related decline in their muscle mass and force [58]. Our finding in ismcTnT-KI mice strongly indicated a causal effect of cTnT overexpression in skeletal muscle on muscle degeneration and function decline, which is mainly mediated through an activated autoimmune response. The smaller NMJ size with reduced PKA-RI $\alpha$  at NMJ and increased denervation are also consistent with our previous findings in the skeletal muscle of aging mice [42].

While these experiments focused on cTnT, it is not the only skeletal muscle autoantigen to exist in the aged muscle, as we have also detected anti-TnT3 autoantibodies in the plasma of older adults. Given

TnT3 is fast muscle fiber specific, this TnT3-targeted autoimmune response may underlie fast skeletal muscle fiber degeneration with aging, which are known to be more affected (e.g., susceptible to atrophy and denervation) with age across species [98–101]. The aging-related myofiber membrane stability decline is muscle type, and potentially fiber type specific [24]. It is possible that cTnT is mainly upregulated in fast fibers with aging as we found out earlier [42], which may interfere with membrane stability potentially through its reported interaction with dystrophin [94], and thus leads to increased membrane permeability in TnT3-positive fast myofibers. Consistently, we have noticed that some of the cTnT and IgG-infiltrated myofibers in aged mice showed dramatically reduced dystrophin on their membrane. In addition, altered myofiber shape and membrane morphology with smaller fiber size were also observed in the ismcTnT-KI mice. Other skeletal muscle proteins could also be the autoantigens that are targeted in the skeletal muscle of older adults. For instance, titin and ryanodine receptor antibodies are mainly present in MG patients over the age of 50–60 years and anti-titin and anti-ryanodine receptor consist mostly of the IgG1 subclass, which is capable of complement activation [102]. Whether these anti-titin and anti-ryanodine receptor and other autoantibodies also exist in normal older adults and contribute to age-related declines in muscle size and function still need to be determined. Autoantibodies against other extracellular matrix protein essential for NMJ formation and maintenance, e.g., agrin and LRP4 autoantibodies, have been found in MG patients [103]. Given that skeletal NMJ degradation increases with age [24, 104, 105], and C-terminal fragments of agrin have been found in blood of older adults with sarcopenia [106–108], it is also possible that agrin and other NMJ associated protein targeting autoantibodies could exist in older adults and serve as specific biomarkers of a subset of sarcopenia patients [108].

#### Translational significance and future directions

Our detection of anti-cTnT autoantibodies in the plasma of older adults is consistent with previous findings [43, 44]. An age-dependent increase of cTnT gene expression in human skeletal muscle has been observed in a cohort study (GSE28422, NCBI GEO dataset) [41]. In addition, a study on 4986



MESA subjects further revealed an age-dependent increase of circulating cTnT in both sexes [109] and cTnT in blood is detectable in elderly patients without clinical diagnosed cardiovascular disease [110]. TnT1 and TnT3 were also reported to be present in circulation of older adults, which are leaked from muscle fibers with increased fiber membrane permeability [111]. Our finding showed the first evidence supporting an important role of autoimmunity in age-related decreases in strength and physical performance. Future cohort studies on larger population will help further determine the prevalence of autoimmunity underlying sarcopenia, and determine if autoimmune-related muscle and blood biomarkers are useful for diagnostics and prediction of changes in strength and performance over time. More skeletal muscle autoantigens could be determined by expression library screening [112, 113] or SEREX technology [114, 115]. Previous studies indicated that mouse heart muscle is spared by recombinant cTnT from an induced autoimmune reaction [116]. This could be related to specificity of epitope and IgG subclass [117] and of conformational epitopes formed by cTnI and cTnT, which exist in heart but not skeletal muscle [118]. It is also possible that cTnT in skeletal muscle is a different alternative splicing form [119–122] (and/or with different post-translational modifications [123]) from that in heart muscle. IgG can activate C3 but it can also activate CDCC or ADCC through macrophages and NK cells or can bind to its antigen and alter function directly [124], which could also be in a IgG subclass specific manner [125]. Further defining these detailed mechanisms in human and mice models will help developing personalized intervention, including but not limited to complement targeted therapy [126, 127], B cell–targeted therapy [128], and epitope mapping [129–131] to inform the discovery and development of new therapeutics to prevent or delay age-related declines in strength and physical performance.

**Acknowledgements** We thank Dr. Carol Milligan and Dr. Osvaldo Delbono for reading and discussing the paper.

**Funding** This work was supported by the R21AG059180 and R21AG060037 (T. Z.), Wake Forest Claude D. Pepper Older Americans Independence Center P30-AG21332 (S. K.), and R01AG020583 (B. N.). Medifast provided the meal replacements used in the SILVER study, which was supported by Wake Forest Claude D. Pepper Older Americans Independence

Center and Wake Forest University Translational Science Center.

**Data availability** The authors confirm that the data supporting the findings of this study are available within the article and/or its [supplementary materials](#).

**Code availability** Not applicable.

## Declarations

**Ethics approval** All subjects gave their informed consent for inclusion before they participated in the IMFIT and SILVER studies.

**Consent to participate** Both IMFIT and SILVER studies were approved by the Wake Forest Institutional Review Board and all participants signed informed consent to participate in the study.

**Consent for publication** All study participants consent for publication of data generate from the IMFIT and SILVER studies.

**Competing interests** The authors declare no competing interests.

## References

1. Hirvensalo M, Rantanen T, Heikkinen E. Mobility difficulties and physical activity as predictors of mortality and loss of independence in the community-living older population. *J Am Geriatr Soc.* 2000;48(5):493–8.
2. Branch LG, Jette AM. A prospective-study of long-term care institutionalization among the aged. *Am J Public Health.* 1982;72(12):1373–9.
3. Muley SA, Day JW. Autoimmune rippling muscle. *Neurology.* 2003;61(6):869–70.
4. Smith RG, et al. Altered muscle calcium-channel binding-kinetics in autoimmune motoneuron disease. *Muscle Nerve.* 1995;18(6):620–7.
5. Ludatscher R, Lichtig C. The muscle capillaries basement-membrane in autoimmune-diseases. *Ultramicroscopy.* 1987;23(2):243–243.
6. Vincent A, Leite MI. Neuromuscular junction autoimmune disease: muscle specific kinase antibodies and treatments for myasthenia gravis. *Curr Opin Neurol.* 2005;18(5):519–25.
7. Liyanage Y, et al. The agrin/muscle-specific kinase pathway: new targets for autoimmune and genetic disorders at the neuromuscular junction. *Muscle Nerve.* 2002;25(1):4–16.
8. Guttsches A, et al. Autoimmune rippling muscle disease: IgG antibodies bind to human muscle fibers. *Neuromuscul Disord.* 2016;26:S203–S203.

9. Koneczny I, et al. IgG4 autoantibodies against muscle-specific kinase undergo Fab-arm exchange in myasthenia gravis patients. *J Autoimmun.* 2017;77:104–15.
10. Rott T, et al. IgG heavy-chain deposition disease affecting kidney, skin, and skeletal muscle. *Nephrol Dial Transplant.* 1998;13(7):1825–8.
11. Klooster R, et al. Muscle-specific kinase myasthenia gravis IgG4 autoantibodies cause severe neuromuscular junction dysfunction in mice. *Brain.* 2012;135:1081–101.
12. Huijbers MG, et al. MuSK IgG4 autoantibodies cause myasthenia gravis by inhibiting binding between MuSK and Lrp4. *Proc Natl Acad Sci USA.* 2013;110(51):20783–8.
13. Isenberg DA. Immunoglobulin deposition in skeletal muscle in primary muscle disease. *Quarterly Journal of Medicine.* 1983;52(207):297–310.
14. Newsom-Davis J. Autoimmune and genetic disorders at the neuromuscular junction. The 1997 Ronnie Mac Keith lecture. *Dev Med Child Neurol.* 1998;40(3):199–206.
15. Voss B, et al. Target proteins in human autoimmune rippling muscle disease. *FASEB J.* 2006;20(4):A30–A30.
16. Bai YH, Pachner AR, Cadavid D. Immunoglobulin deposition and inflammation in skeletal muscle in the nonhuman primate model of Lyme borreliosis. *Ann Neurol.* 2002;52(3):S94–S94.
17. Tuzun E, et al. Increased complement consumption in MuSK-antibody-positive myasthenia gravis patients. *Med Princ Pract.* 2011;20(6):581–3.
18. Suzuki S, et al. Autoimmune targets of heart and skeletal muscles in myasthenia gravis. *Arch Neurol.* 2009;66(11):1334–8.
19. Romi F, Aarli JA, Gilhus NE. Myasthenia gravis patients with ryanodine receptor antibodies have distinctive clinical features. *Eur J Neurol.* 2007;14(6):617–20.
20. Rimer M. Agrin-induced aggregation of acetylcholine receptors in muscles of rats with experimental autoimmune myasthenia gravis. *Myasthenia Gravis Relat Dis.* 1998;841:546–9.
21. Heckmann JM, et al. Human muscle acetylcholine receptor alpha-subunit gene (CHRNA1) association with autoimmune myasthenia gravis in black, mixed-ancestry and Caucasian subjects. *J Autoimmun.* 1996;9(2):175–80.
22. Straub V, et al. Animal models for muscular dystrophy show different patterns of sarcolemmal disruption. *J Cell Biol.* 1997;139(2):375–85.
23. Roche JA, et al. Myofiber damage precedes macrophage infiltration after in vivo injury in dysferlin-deficient A/J mouse skeletal muscle. *Am J Pathol.* 2015;185(6):1686–98.
24. Hughes DC, et al. Age-related differences in dystrophin: impact on force transfer proteins, membrane integrity, and neuromuscular junction stability. *J Gerontol A Biol Sci Med Sci.* 2017;72(5):640–8.
25. Morgan JE, et al. Necroptosis mediates myofiber death in dystrophin-deficient mice. *Nat Commun.* 2018;9(1):3655.
26. Schreiber A, et al. Necroptosis controls NET generation and mediates complement activation, endothelial damage, and autoimmune vasculitis. *Proc Natl Acad Sci USA.* 2017;114(45):E9618–25.
27. Watad A, et al. Autoimmunity in the elderly: insights from basic science and clinics - a mini-review. *Gerontology.* 2017;63(6):515–23.
28. Prelog M. Aging of the immune system: a risk factor for autoimmunity? *Autoimmun Rev.* 2006;5(2):136–9.
29. Degreef GE, et al. Serum immunoglobulin class and IgG subclass levels and the occurrence of homogeneous immunoglobulins during the course of aging in humans. *Mech Ageing Dev.* 1992;66(1):29–44.
30. Listi F, et al. A study of serum immunoglobulin levels in elderly persons that provides new insights into B cell immunosenescence. *Estrogens Hum Dis.* 2006;1089:487–95.
31. Batory G, et al. Antibody and immunoglobulin levels in aged humans. *Arch Gerontol Geriatr.* 1984;3(2):175–88.
32. Radl J, et al. Immunoglobulin patterns in humans over 95 years of age. *Clin Exp Immunol.* 1975;22(1):84–90.
33. Jones G, et al. Genome-wide meta-analysis of muscle weakness identifies 15 susceptibility loci in older men and women. *Nat Commun.* 2021;12(1):654.
34. Perry SV. Troponin T: genetics, properties and function. *J Muscle Res Cell Motil.* 1998;19(6):575–602.
35. Fredericks S, et al. Effect of denervation on the content of cardiac troponin-T and cardiac troponin-I in rat skeletal muscle. *Clin Biochem.* 2007;40(5–6):423–6.
36. Saggin L, et al. Cardiac troponin T in developing, regenerating and denervated rat skeletal muscle. *Development.* 1990;110(2):547–54.
37. Jaffe AS, et al. Diseased skeletal muscle: a noncardiac source of increased circulating concentrations of cardiac troponin T. *J Am Coll Cardiol.* 2011;58(17):1819–24.
38. Rittoo D, et al. Elevation of cardiac troponin T, but not cardiac troponin I, in patients with neuromuscular diseases. *J Am Coll Cardiol.* 2014;63(22):2411–20.
39. Dadgar S, et al. Asynchronous remodeling is a driver of failed regeneration in Duchenne muscular dystrophy. *J Cell Biol.* 2014;207(1):139–58.
40. Bakay M, et al. Nuclear envelope dystrophies show a transcriptional fingerprint suggesting disruption of Rb-MyoD pathways in muscle regeneration. *Brain.* 2006;129:996–1013.
41. Raue U, et al. Transcriptome signature of resistance exercise adaptations: mixed muscle and fiber type specific profiles in young and old adults. *J Appl Physiol (1985).* 2012;112(10):1625–36.
42. Xu ZR, et al. Cardiac troponin T and fast skeletal muscle denervation in ageing. *J Cachexia Sarcopenia Muscle.* 2017;8(5):808–23.
43. Adamczyk M, Brashear RJ, Mattingly PG. Coprevalence of autoantibodies to cardiac troponin I and T in normal blood donors. *Clin Chem.* 2010;56(4):676–7.
44. Adamczyk M, Brashear RJ, Mattingly PG. Prevalence of autoantibodies to cardiac troponin T in healthy blood donors. *Clin Chem.* 2009;55(8):1592–3.
45. Feng HZ, et al. Toad heart utilizes exclusively slow skeletal muscle troponin T an evolutionary adaptation with potential functional benefits. *J Biol Chem.* 2012;287(35):29753–64.

46. Zhang T, et al. Human slow troponin T (TNNT1) Pre-mRNA Alternative Splicing Is an Indicator of Skeletal Muscle Response to Resistance Exercise in Older Adults. *J Gerontol A Biol Sci Med Sci*. 2014;69(12):1437–47.
47. Nicklas BJ, et al. Effects of resistance training with and without caloric restriction on physical function and mobility in overweight and obese older adults: a randomized controlled trial. *Am J Clin Nutr*. 2015;101(5):991–9.
48. Beavers KM, et al. Effect of protein source during weight loss on body composition, cardiometabolic risk and physical performance in abdominally obese, older adults: a pilot feeding study. *J Nutr Health Aging*. 2015;19(1):87–95.
49. Guralnik JM, et al. A short physical performance battery assessing lower extremity function: association with self-reported disability and prediction of mortality and nursing home admission. *J Gerontol*. 1994;49(2):M85–94.
50. Martin HJ, et al. Is hand-held dynamometry useful for the measurement of quadriceps strength in older people? A comparison with the gold standard Bodex dynamometry. *Gerontology*. 2006;52(3):154–9.
51. McCarthy JJ, et al. Inducible Cre transgenic mouse strain for skeletal muscle-specific gene targeting. *Skelet Muscle*. 2012;2(1):8.
52. Madisen L, et al. A robust and high-throughput Cre reporting and characterization system for the whole mouse brain. *Nat Neurosci*. 2010;13(1):133–40.
53. Sohail DS, et al. Temporally regulated and tissue-specific gene manipulations in the adult and embryonic heart using a tamoxifen-inducible Cre protein. *Circ Res*. 2001;89(1):20–5.
54. Livak KJ, Schmittgen TD. Analysis of relative gene expression data using real-time quantitative PCR and the 2(-Delta Delta C(T)) Method. *Methods*. 2001;25(4):402–8.
55. Files DC, et al. Therapeutic exercise attenuates neutrophilic lung injury and skeletal muscle wasting. *Sci Transl Med*. 2015;7(278):278ra32.
56. Arimura S, et al. Neuromuscular disease. DOK7 gene therapy benefits mouse models of diseases characterized by defects in the neuromuscular junction. *Science*. 2014;345(6203):1505–8.
57. Xu Z, et al. Cardiac troponin T and fast skeletal muscle denervation in ageing. *J Cachexia Sarcopenia Muscle*. 2017;8(5):808–23.
58. Graber TG, et al. C57BL/6 neuromuscular health-span scoring system. *J Gerontol A Biol Sci Med Sci*. 2013;68(11):1326–36.
59. Koutakis P, et al. Abnormal myofiber morphology and limb dysfunction in claudication. *J Surg Res*. 2015;196(1):172–9.
60. Schaeffer L, de Kerchovd'Exaerde A, Changeux JP. Targeting transcription to the neuromuscular synapse. *Neuron*. 2001;31(1):15–22.
61. Mejat A, et al. Synapse-specific gene expression at the neuromuscular junction. *Myasthenia Gravis and Related Disorders*. 2003;998:53–65.
62. Zhu XJ, Yeadon JE, Burden SJ. Aml1 is expressed in skeletal-muscle and is regulated by innervation (Vol 14, Pg 8056, 1994). *Mol Cell Biol*. 1995;15(2):1136–1136.
63. Wang XX, et al. Runx1 prevents wasting, myofibrillar disorganization, and autophagy of skeletal muscle. *Genes Dev*. 2005;19(14):1715–22.
64. Pestronk A, et al. Immune myopathy with large histiocyte-related myofiber necrosis. *Neurology*. 2019;92(15):e1763–72.
65. Colonna-Romano G, et al. B cell immunosenescence in the elderly and in centenarians. *Rejuvenation Res*. 2008;11(2):433–9.
66. Drachman DB. *Myasthenia gravis*. *N Engl J Med*. 1994;330(25):1797–810.
67. Vincent A. Unravelling the pathogenesis of myasthenia gravis. *Nat Rev Immunol*. 2002;2(10):797–804.
68. McConville J, et al. Detection and characterization of MuSK antibodies in seronegative myasthenia gravis. *Ann Neurol*. 2004;55(4):580–4.
69. Shiraishi H, et al. Acetylcholine receptors loss and post-synaptic damage in MuSK antibody-positive myasthenia gravis. *Ann Neurol*. 2005;57(2):289–93.
70. Ludwig RJ, et al. Mechanisms of autoantibody-induced pathology. *Front Immunol*. 2017;8:603.
71. Plomp JJ, et al. Pathogenic IgG4 subclass autoantibodies in MuSK myasthenia gravis. *Ann N Y Acad Sci*. 2012;1275:114–22.
72. Naito AT, et al. Complement C1q activates canonical wnt signaling and promotes aging-related phenotypes. *Cell*. 2012;149(6):1298–313.
73. Watanabe S, et al. Serum C1q as a novel biomarker of sarcopenia in older adults. *FASEB J*. 2015;29(3):1003–10.
74. Noris M, Remuzzi G. Overview of complement activation and regulation. *Semin Nephrol*. 2013;33(6):479–92.
75. Ricklin D, et al. Complement component C3-The “Swiss Army Knife” of innate immunity and host defense. *Immunol Rev*. 2016;274(1):33–58.
76. Kusner LL, Kaminski HJ. The role of complement in experimental autoimmune myasthenia gravis. *Myasthenia Gravis Relat Disord I*. 2012;1274:127–32.
77. Nesargikar PN, Spiller B, Chavez R. The complement system: history, pathways, cascade and inhibitors. *Eur J Microbiol Immunol (Bp)*. 2012;2(2):103–11.
78. Wu X, et al. Complement C3 deficiency ameliorates aging related changes in the kidney. *Life Sci*. 2020;260:118370.
79. Shi Q, et al. Complement C3-deficient mice fail to display age-related hippocampal decline. *J Neurosci*. 2015;35(38):13029–42.
80. Han R, et al. Genetic ablation of complement C3 attenuates muscle pathology in dysferlin-deficient mice. *J Clin Invest*. 2010;120(12):4366–74.
81. Wang JY, et al. Caspase-3 cleavage of dishevelled induces elimination of postsynaptic structures. *Dev Cell*. 2014;28(6):670–84.
82. Zhu HP, Pytel P, Gomez CM. Selective inhibition of caspases in skeletal muscle reverses the apoptotic synaptic degeneration in slow-channel myasthenic syndrome. *Hum Mol Genet*. 2014;23(1):69–77.

83. Frenette J, Cai BY, Tidball JG. Complement activation promotes muscle inflammation during modified muscle use. *Am J Pathol.* 2000;156(6):2103–10.
84. Shi H, et al. Exposure to the complement C5b–9 complex sensitizes 661W photoreceptor cells to both apoptosis and necroptosis. *Apoptosis.* 2015;20(4):433–43.
85. Carter AM. Complement activation: an emerging player in the pathogenesis of cardiovascular disease. *Scientifica (Cairo).* 2012;2012:402783.
86. Liu ZF, et al. Elevated serum complement factors 3 and 4 are strong inflammatory markers of the metabolic syndrome development: a longitudinal cohort study. *Sci Rep.* 2016;6:18713.
87. Chamberlain-Banoub J, et al. Complement membrane attack is required for endplate damage and clinical disease in passive experimental myasthenia gravis in Lewis rats. *Clin Exp Immunol.* 2006;146(2):278–86.
88. El Idrissi NB, et al. Complement activation at the motor end-plates in amyotrophic lateral sclerosis. *J Neuroinflammation.* 2016;13(1):72.
89. Rojana-udomsart A, et al. Complement-mediated muscle cell lysis: A possible mechanism of myonecrosis in anti-SRP associated necrotizing myopathy (ASANM). *J Neuroimmunol.* 2013;264(1–2):65–70.
90. Alissafi T, et al. Mitochondrial oxidative damage underlies regulatory T cell defects in autoimmunity. *Cell Metab.* 2020;32(4):591–604.e7.
91. Engel AG, Arahata K. The membrane attack complex of complement at the endplate in myasthenia-gravis. *Ann N Y Acad Sci.* 1987;505:326–32.
92. Zhang T, Birbrair A, Delbono O. Nonmyofibrillar-associated troponin T3 nuclear and nucleolar localization sequence and leucine zipper domain mediate muscle cell apoptosis. *Cytoskeleton (Hoboken).* 2013;70(3):134–47.
93. Jeong EM, et al. Nonmyofibrillar-associated troponin T fragments induce apoptosis. *Am J Physiol Heart Circ Physiol.* 2009;297(1):H283–92.
94. Sumandea CA, et al. Cardiac troponin T, a sarcomeric AKAP, tethers protein kinase A at the myofilaments. *J Biol Chem.* 2011;286(1):530–41.
95. Chai RJ, et al. Striking denervation of neuromuscular junctions without lumbar motoneuron loss in geriatric mouse muscle. *Plos One.* 2011;6(12).
96. Brooks SV, Faulkner JA. Contractile properties of skeletal muscles from young, adult and aged mice. *J Physiol.* 1988;404:71–82.
97. Lynch GS, et al. Force and power output of fast and slow skeletal muscles from mdx mice 6–28 months old. *J Physiol.* 2001;535(Pt 2):591–600.
98. Feng X, et al. Myosin heavy chain isoform expression in the Vastus Lateralis muscle of aging African green vervet monkeys. *Exp Gerontol.* 2012;47(8):601–7.
99. Valdez G, et al. Shared resistance to aging and ALS in neuromuscular junctions of specific muscles. *PLoS One.* 2012;7(4):e34640.
100. Ciciliot S, et al. Muscle type and fiber type specificity in muscle wasting. *Int J Biochem Cell Biol.* 2013;45(10):2191–9.
101. Nilwik R, et al. The decline in skeletal muscle mass with aging is mainly attributed to a reduction in type II muscle fiber size. *Exp Gerontol.* 2013;48(5):492–8.
102. Romi F, et al. Complement activation by titin and ryandine receptor autoantibodies in myasthenia gravis - a study of IgG subclasses and clinical correlations. *J Neuroimmunol.* 2000;111(1–2):169–76.
103. Gasperi C, et al. Anti-agrin autoantibodies in myasthenia gravis. *Neurology.* 2014;82(22):1976–83.
104. Deschenes MR, et al. Remodeling of the neuromuscular junction precedes sarcopenia related alterations in myofibers. *Exp Gerontol.* 2010;45(5):389–93.
105. Rowan SL, et al. Denervation causes fiber atrophy and myosin heavy chain co-expression in senescent skeletal muscle. *PLoS One.* 2012;7(1):e29082.
106. Drey M, et al. C-terminal agrin fragment as a potential marker for sarcopenia caused by degeneration of the neuromuscular junction. *Exp Gerontol.* 2013;48(1):76–80.
107. Pratt J, et al. Plasma C-terminal agrin fragment as an early biomarker for sarcopenia: results from the GenoFit study. *J Gerontol A Biol Sci Med Sci.* 2021;76(12):2090–6.
108. Hettwer S, et al. Elevated levels of a C-terminal agrin fragment identifies a new subset of sarcopenia patients. *Exp Gerontol.* 2013;48(1):69–75.
109. Seliger SL, et al. High-sensitive cardiac troponin T as an early biochemical signature for clinical and subclinical heart failure MESA (Multi-Ethnic Study of Atherosclerosis). *Circulation.* 2017;135(16):1494–505.
110. Zhang SJ, et al. High-sensitivity cardiac troponin T in geriatric inpatients. *Arch Gerontol Geriatr.* 2016;65:111–5.
111. Abreu EL, et al. Skeletal muscle troponin as a novel biomarker to enhance assessment of the impact of strength training on fall prevention in the older adults. *Nurs Res.* 2014;63(2):75–82.
112. Watkins TC, et al. Identification of skeletal muscle autoantigens by expression library screening using sera from autoimmune rippling muscle disease (ARMMD) patients. *J Cell Biochem.* 2006;99(1):79–87.
113. Jadali Z, Sanati MH. The autoimmune diseases manifested by production of autoantibodies: the autoantigens identified by random peptide library. *Iran J Allergy Asthma Immunol.* 2008;7(3):115–31.
114. Wang KJ, et al. Identification of tumor-associated antigens by using SEREX in hepatocellular carcinoma. *Cancer Lett.* 2009;281(2):144–50.
115. Hao S, et al. Screening novel autoantigens targeted by serum IgG autoantibodies in immunorelated pancytopenia by SEREX. *Int J Hematol.* 2017;106(5):622–30.
116. Goser S, et al. Cardiac troponin I but not cardiac troponin T induces severe autoimmune inflammation in the myocardium. *Circulation.* 2006;114(16):1693–702.
117. Savukoski T, et al. Epitope specificity and IgG subclass distribution of autoantibodies to cardiac troponin. *Clin Chem.* 2013;59(3):512–8.
118. Vylegzhanina AV, et al. Anti-cardiac troponin autoantibodies are specific to the conformational epitopes formed by cardiac troponin I and troponin T in the Ternary troponin complex. *Clin Chem.* 2017;63(1):343–50.

119. Zhang T, et al. Human Slow Troponin T (TNNT1) Pre-mRNA alternative splicing is an indicator of skeletal muscle response to resistance exercise in older adults. *J Gerontol Ser A Biol Sci Med Sci*. 2014;69(12):1437–47.
120. Marden JH, et al. Alternative splicing, muscle contraction and intraspecific variation: associations between troponin T transcripts, Ca(2+) sensitivity and the force and power output of dragonfly flight muscles during oscillatory contraction. *J Exp Biol*. 2001;204(Pt 20):3457–70.
121. Farza H, et al. Genomic organisation, alternative splicing and polymorphisms of the human cardiac troponin T gene. *J Mol Cell Cardiol*. 1998;30(6):1247–53.
122. Biesiadecki BJ, et al. Cardiac troponin T variants produced by aberrant splicing of multiple exons in animals with high instances of dilated cardiomyopathy. *J Biol Chem*. 2002;277(52):50275–85.
123. Sheng JJ, Jin JP. Gene regulation, alternative splicing, and posttranslational modification of troponin subunits in cardiac development and adaptation: a focused review. *Front Physiol*. 2014;5:165.
124. Tang Y, et al. Regulation of antibody-dependent cellular cytotoxicity by IgG intrinsic and apparent affinity for target antigen. *J Immunol*. 2007;179(5):2815–23.
125. Vidarsson G, Dekkers G, Rispens T. IgG subclasses and allotypes: from structure to effector functions. *Front Immunol*. 2014;5:520.
126. Zipfel PF, et al. Complement inhibitors in clinical trials for glomerular diseases. *Front Immunol*. 2019;10:2166.
127. Albazli K, Kaminski HJ, Howard JF. Complement inhibitor therapy for myasthenia gravis. *Front Immunol*. 2020;11:917.
128. Stubgen JP. B cell-targeted therapy with rituximab and autoimmune neuromuscular disorders. *J Neuroimmunol*. 2008;204(1–2):1–12.
129. Gershoni JM, et al. Epitope mapping: the first step in developing epitope-based vaccines. *BioDrugs*. 2007;21(3):145–56.
130. Casina VC, et al. High-resolution epitope mapping by HX MS reveals the pathogenic mechanism and a possible therapy for autoimmune TTP syndrome. *Proc Natl Acad Sci U S A*. 2015;112(31):9620–5.
131. Agnolon V, et al. ELISA assay employing epitope-specific monoclonal antibodies to quantify circulating HER2 with potential application in monitoring cancer patients undergoing therapy with trastuzumab. *Sci Rep*. 2020;10(1):3016.

**Publisher's note** Springer Nature remains neutral with regard to jurisdictional claims in published maps and institutional affiliations.